BASIC SCIENCE

Nanomedicine: Nanotechnology, Biology, and Medicine
7 (2011) 904–913

Research Article

nanomedjournal.com

ZnO nanorod-induced apoptosis in human alveolar adenocarcinoma cells via p53, survivin and bax/bcl-2 pathways: role of oxidative stress

Maqusood Ahamed, PhD[a,*], Mohd Javed Akhtar, MSc[b], Mohan Raja, PhD[a], Iqbal Ahmad, PhD[b], Mohammad Kaleem Javed Siddiqui, PhD[c], Mohamad S. AlSalhi, PhD[a], Salman A. Alrokayan, PhD[a]

[a]*King Abdullah Institute for Nanotechnology, King Saud University, Riyadh, Saudi Arabia*
[b]*Fibre Toxicology Division, Indian Institute of Toxicology Research, Lucknow, India*
[c]*Council of Science and Technology - Uttar Pradesh, Lucknow, India*

Received 8 November 2010; accepted 19 April 2011

Abstract

Zinc oxide (ZnO) nanoparticles (NPs) are increasingly recognized for their utility in biological applications, including biosensor and medicine. However, little is known about the toxicity mechanisms of ZnO nanorods in human cells. This study was designed to investigate the possible mechanisms of apoptosis induced by ZnO nanorods in human alveolar adenocarcinoma (A549) cells. ZnO nanorod was found to induce cytotoxicity, reactive oxygen species (ROS) generation, oxidative stress and activities of caspase-3 & caspase-9 in a dose- and time-dependent manner. Western blot results showed that ZnO nanorods induced the expression of heat shock protein 70, a first-tier marker of cell damage and a cell-cycle checkpoint protein p53. Moreover, pro-apoptotic protein bax was upregulated and the antiapoptotic proteins, survivin and bcl-2, were downregulated in ZnO nanorod exposed cells. In conclusion, our data demonstrateas that ZnO nanorod induced apoptosis in A549 cells through ROS and oxidative stress via p53, survivin, bax/bcl-2 and caspase pathways.

From the Clinical Editor: This study describes the mechanisms of apoptosis induced by ZnO nanorods in human alveolar adenocarcinoma cells.

Key words: ZnO nanorods; Oxidative stress; Apoptosis; Survivin; p53

Nanoscale zinc oxide (nZnO) is increasingly used in catalysis, electronics, clothing, paints, sunscreens and cosmetics.[1-3] Current interest of nZnO has been focused on its biological applications, including as biosensor and in medicine.[4-6] These broad applications, however, increase human and environmental exposure and thus the potential risk related to their short- and long-term toxicity. There are studies reporting the cytotoxic potential of nZnO in mammalian cells.[7-9] Toxicity of nZnO to bacteria, microalgae, protozoa, yeast and zebrafish is also shown by investigators.[10-12] Some of these studies provided evidence that the cytotoxicity of nZnO was mediated through reactive oxygen species (ROS) generation and oxidative stress.[9,13] In addition, a few recent studies showed the genotoxicity of nZnO in human cells.[14,15] For example, Sharma et al[14] reported that nZnO induced DNA damage in human epidermal cells, which may be mediated through lipid peroxidation and oxidative stress. Lin et al[15] found that nZnO induced oxidative DNA damage in human lung epithelial cells. Information, however, about mechanisms of apoptosis induced by nZnO is largely lacking.

Several proteins are known to sense DNA damage and apoptosis. The tumor-suppressor protein p53 is able to activate cell-cycle checkpoints, DNA repair and apoptosis response to maintain genomic stability.[16] In the presence of DNA damage or cellular stress, p53 protein triggers cell-cycle arrest to provide time for the damage to be repaired or for self-mediated apoptosis.[16] Survivin, an inhibitor of apoptosis, has recently been reported to play an important role in both cell proliferation and apoptosis.[17] Downregulation of survivin may cause a cell-cycle defect that leads to apoptosis. The bcl-2 protein has an antiapoptotic effect, whereas the bax is known for pro-apoptotic

Conflict of interest statement. The authors declare that there are no conflicts of interest.

Funding source. King Abdullah Institute for Nanotechnology (KAIN). The authors received research funding from King Abdulaziz City for Science and Technology (KACST) under the National Plan for Science and Technology (NPST) (Grant No.: 10-NAN1201-02).

*Corresponding author: King Abdullah Institute for Nanotechnology, King Saud University, Riyadh-11451, Saudi Arabia.

E-mail address: maqusood@gmail.com (M. Ahamed).

1549-9634/$ – see front matter © 2011 Elsevier Inc. All rights reserved.
doi:10.1016/j.nano.2011.04.011

activity.[18] A critical ratio of bax/bcl-2 proteins plays a major role in mitochondrial outer-membrane permeabilization, release of cytochrome C in the cytosol and, thus, initiation of apoptosis.[19]

In view of the significant lack of information about the mechanisms of nZnO toxicity, this study was designed to investigate the possible mechanisms of apoptosis induced by ZnO nanorods in human alveolar adenocarcinoma (A549) cells through oxidative stress via p53, survivin and bax/bcl-2 pathways. Recent studies have shown that nZnO releases zinc ions (Zn^{2+}) in the aqueous state.[10,11] Therefore, we also determined whether ZnO nanorods induce a cellular response in A549 cells, and, if so, how they produce toxicity by releasing soluble Zn^{2+} or by exerting a toxic effect unique to ZnO nanorods.

Methods

Reagents

Fetal bovine serum (FBS), penicillin-streptomycin, DMEM/F-12 medium and HBSS were purchased from Invitrogen Co. (Carlsbad, California), 3-(4,5-dimethylthiazol-2-yl)-2,5 diphenyltetrazolium bromide (MTT), 2,7-dichlorofluorescin diacetate (DCFH-DA), reduced glutathione (GSH), 5,5-dithio-bis-(2-nitrobenzoic acid) (DTNB), thiobarbituric acid (TBA), anti-p53 monoclonal antibody, anti-survivin (BIRC5) polyclonal antibody, anti-bax monoclonal antibody, anti-bcl-2 monoclonal antibody and anti-β actin monoclonal antibody were obtained from Sigma-Aldrich (St. Louis, Missouri). Secondary antibodies and RIPA buffer were bought from Santa Cruz Biotechnologies, Inc., (Santa Cruz, California). All other chemicals used were of the highest purity available from commercial sources.

Synthesis of ZnO nanorods

ZnO nanorods were prepared via sol-gel chemistry using zinc acetate dihydrate [$(CH_3\ COO)_2$ Zn.2H2O, 99.0-101%, Merck Chemicals, Darmstadt, Germany] as a precursor with sodium hydroxide solution through microemulsion technique as described in our previous publication.[20]

Characterization of ZnO nanorods

The crystalline nature of prepared ZnO nanorods was carried out by taking x-ray diffraction (XRD) pattern at 25–28°C with a PANalytical X'Pert x-ray diffractometer equipped with a nickel (Ni) filtered using Cu Kα (λ = 1.54056 Å) radiations as the x-ray source. Morphology and size of ZnO nanorods were examined by field emission scanning electron microscope (FESEM, JSM-7600F, JEOL, Inc., Tokyo, Japan) and field emission transmission electron microscopy (FETEM, JEM-2100F, JEOL Inc.) at an accelerating voltage of 15 kV and 200 kV, respectively. To check the purity of ZnO nanorods, an energy-dispersive x-ray (EDX) spectroscopy analysis was performed.

Dynamic light scattering (DLS) (ZetaSizer-HT Malvern Instrument, Worcestershire, United Kingdom) was used to determine the hydrodynamic size and zeta potential of the ZnO nanorods suspension in cell culture medium. Dry powder of ZnO nanorods was suspended in cell culture medium at a concentration of 1 mg/ml, and then sonicated using a sonicator bath at room temperature for 15 minutes at 40 W to form a homogeneous suspension. For DLS size measurement, sonicated 1 mg/ml ZnO nanorods stock solution was diluted to 5–100 μg/ml working solutions.

Cell culture and exposure to ZnO nanorods

The human alveolar adenocarcinoma (A549) cells have been used widely in cytotoxicity and genotoxicity studies.[21,22] Cells were cultured in Dulbecco's modified Eagle's medium (DMEM)/F-12 medium supplemented with 10% FBS and 100 U/ml penicillin-streptomycin at 5% CO_2 and 37°C. At the confluency of 85%, cells were trypsinized and subcultured into 75 cm^2 flasks, 6-well plates or 96-well plates according to selection of experiments. Cells were allowed to attach the surface for 24 hours before treatment. ZnO nanorods was suspended in cell culture medium and diluted to appropriate concentrations (0, 5, 10, 25, 50 and 100 μg/ml). The appropriate dilutions of ZnO nanorods were then sonicated using a sonicator bath at room temperature for 10 minutes at 40 W to avoid particles agglomeration before exposure to the cells. Cells not exposed to ZnO nanorods served as control in each experiment.

Analysis of dissolution of ZnO nanorods and exposure of cells with the same

To determine whether Zn^{2+} released from ZnO nanorods suspension may play a role in cellular toxicity, the released Zn^{2+} concentrations were measured in all the culture media collected from ZnO nanorods treatment. Culture media were taken from the ZnO nanorod-treated cells immediately at the end of exposure and centrifuged at 30000*g* for 30 minutes. After centrifugation, the released Zn^{2+} concentrations in the supernatants were detected by graphite furnace atomic absorption spectrometry (GFAA). Moreover, to compare the toxic effects of released Zn^{2+} with ZnO nanorods, another exposure regime with soluble Zn^{2+} was performed. In that case, the ZnO nanorod suspension was replaced by Zn^{2+} solution (10 and 100 μg/ml), which was dosed by adding the required mass of zinc chloride ($ZnCl_2$, 98.0-100.5%, Merck Chemicals) to the culture medium. Criteria for the selection of two concentrations 10 and 100 μg/ml of soluble Zn^{2+} is explained in the Results section of this article.

Mitochondrial function

MTT assay was used to investigate mitochondrial function as described by Mossman[23] with some modifications reported in our previous study.[24] In brief, 1×10^4 cells per well were seeded in 96-well plates and exposed to different concentrations of ZnO nanorods and soluble Zn^{2+} for 24 and 48 hours. After the exposure completed, the culture medium was removed from each well and replaced with 100 μl of new medium containing MTT (0.5 mg/ml) and incubated for 3 hours at 37°C. The resulting formazan product was dissolved by adding equal amount of acidified isopropanol. To minimize the interference in absorbance caused by the turbidity occurring due to NPs, 96-well plates were centrifuged at 2500*g* for 10 minutes. Then, a 100 μl supernatant was transferred to other fresh wells of microtiter

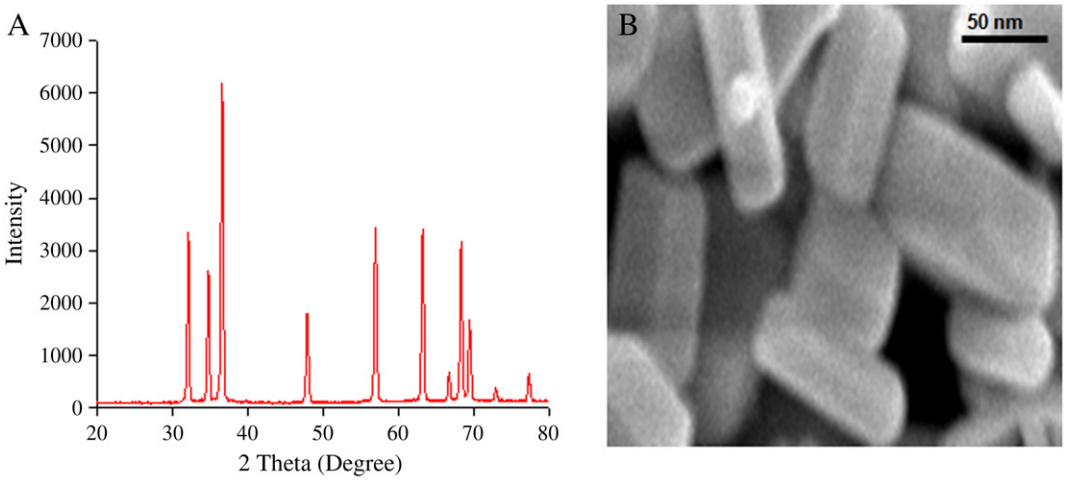

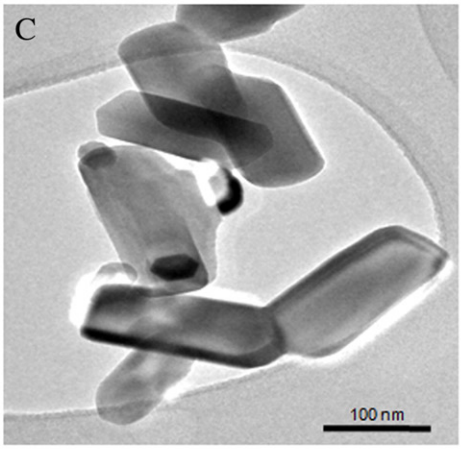

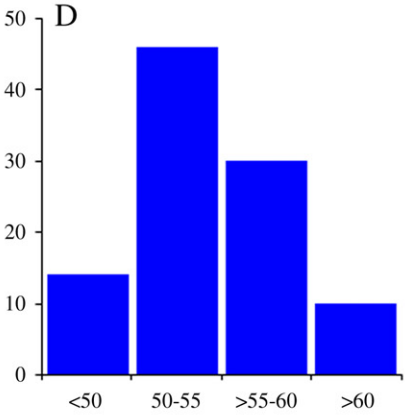

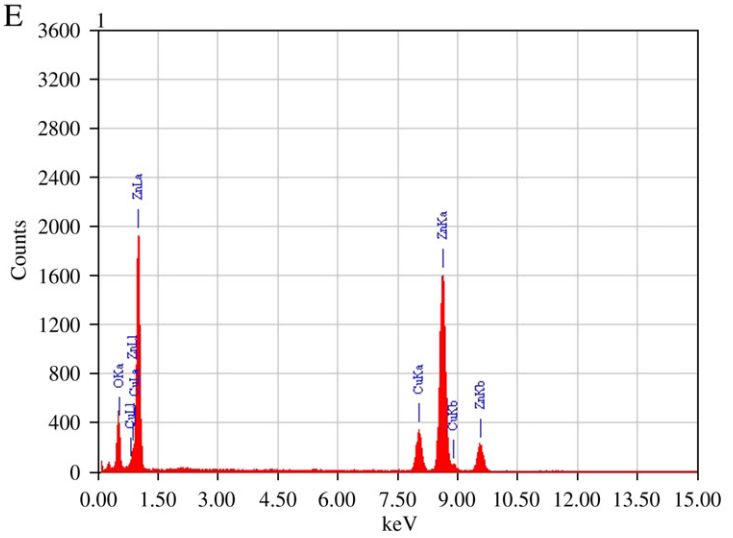

F

DLS size (nm)	Zeta Potential (-mV)
97	-29

Figure 1. Characterization of ZnO nanorods. **(A)** XRD pattern of ZnO nanorods. **(B)** SEM image of ZnO nanorods. **(C)** TEM image of ZnO nanorods. **(D)** Frequency of size distribution of ZnO nanorods analyzed by TEM. **(E)** EDX spectrum of ZnO Nanorods. **(F)** DLS measurement of ZnO nanorods for hydrodynamic size and zeta potential.

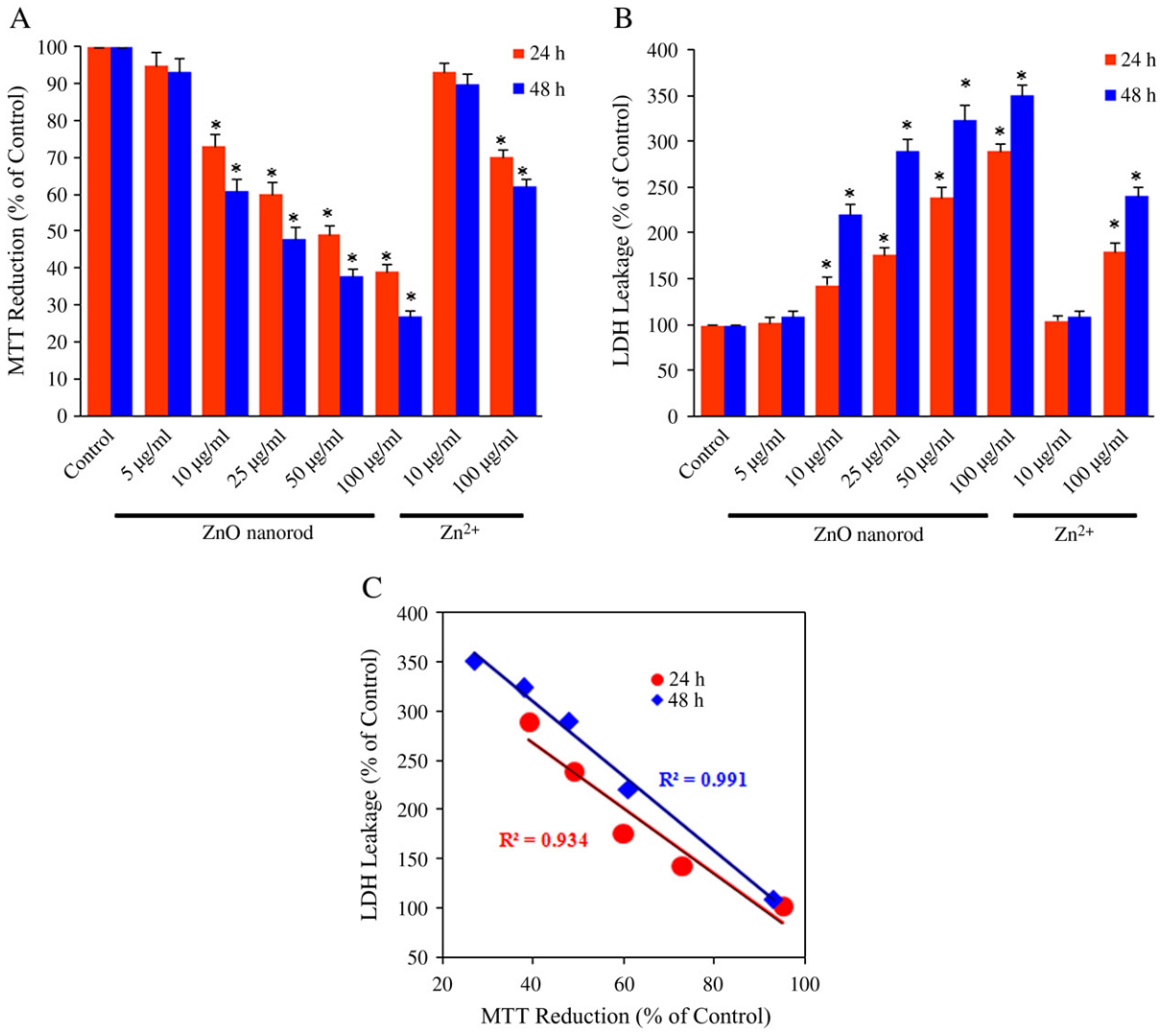

Figure 2. Comparative effects of ZnO nanorods and Zn^{2+} on mitochondrial function (MTT reduction) and membrane damage (LDH leakage) in human alveolar adenocarcinoma cells. Cells were treated with 5, 10, 25, 50 and 100 μg/ml of ZnO nanorods and 10 and 100 μg/ml of Zn^{2+} for 24 and 48 h. At the end of treatment MTT reduction and LDH leakage were determined as described in the materials and methods. **(A)** MTT reduction **(B)** LDH leakage. Data represented are mean ± SD of three identical experiments made in triplicate. *Statistically significant difference in comparison with the controls ($P < 0.05$ for each).

plate and then absorbance was measured at 570 nm by using a microplate reader (Synergy-HT, BioTek Instruments, Winooski, Vermont). Following noncellular background (i.e., a blank, consisting of yellow MTT and acidified isopropanol) subtraction, all data were normalized to the MTT conversion activity of media-treated control cells. This value corresponds to a 0% decrease in MTT conversion activity and represents 100% cell viability.

Lactate dehydrogenase leakage assay

Lactate dehydrogenase (LDH) leakage assay was carried out by the LDH-Cytotoxicity assay kit (BioVision Technologies Inc., Exton, Pennsylvania). In addition, 1×10^4 cells per well were seeded in 96-well plates and exposed to different concentrations of ZnO nanorods and soluble Zn^{2+} for 24 and 48 hours. At the end of treatment, LDH levels in the media versus the cells were quantified and compared with the control values using microplate reader (Synergy-HT, BioTek) at 340 nm, according to the manufacturer's protocol. To minimize the interference in absorbance caused by the turbidity occurring due to ZnO nanorods, the 96-well plates were centrifuged as described above.

Measurement of reactive oxygen species generation

The production of intracellular ROS was measured using 2,7-dichlorofluorescin diacetate (DCFH-DA).[25] The DCFH-DA passively enters the cell where it reacts with ROS to form the highly fluorescent compound dichlorofluorescein (DCF). Briefly, 10 mM DCFH-DA stock solution (in methanol) was diluted in culture medium without serum or other additive to yield a 100 μM working solution. At the end of exposure cells were washed twice with cold HBSS and then incubated in 1 ml working solution of DCFH-DA at 37°C for 30 minutes. Cells were lysed in alkaline solution and centrifuged at 2500*g* for 10 minutes. Then, a 200 μl

supernatant was transferred to the other fresh well of microplates and fluorescence was measured at excitation of 485 nm and emission of 520 nm using a microplate reader (Synergy-HT, BioTek). The values of ROS were expressed as percent of fluorescence intensity relative to controls.

Assays of oxidative stress biomarkers

For the measurement of oxidative-stress biomarkers, cells were cultured in a 75-cm^2 culture flask and exposed to different concentrations of ZnO nanorods and soluble Zn^{2+} for 24 and 48 hours. After the treatment, cells were washed and harvested in ice-cold phosphate buffer saline at 4°C. The harvested cell pellets were then lysed in cell lysis buffer [20 mM Tris-HCl (pH 7.5), 150 mM NaCl, 1 mM Na_2EDTA, 1%Triton and 2.5 mM sodium pyrophosphate]. Following centrifugation (15000*g* for 10 minutes at 4°C) the supernatant (cell extract) was maintained on ice until assayed for oxidative-stress biomarkers.

The extent of membrane lipid peroxidation (LPO) was estimated by measuring the formation of malondialdehyde (MDA) using the method of Ohkawa et al.[26] MDA is one of the products of membrane LPO. A mixture of 0.1 ml cell extract and 1.9 ml of 0.1 M sodium phosphate buffer (pH 7.4) was incubated at 37°C for 1 hour. The incubation mixture, after precipitation with 5% TCA, was centrifuged (2300*g* for 15 minutes at room temperature) and collected the supernatant. Then, 1.0 ml of 1% TBA was added to the supernatant and placed in the boiling water for 15 minutes. After cooling to room temperature, absorbance of the mixture was taken at 532 nm and expressed in nmol MDA/h/mg protein using molar extinction coefficient of 1.56×10^5 M^{-1} cm^{-1}. Glutathione (GSH) level was quantified using Ellman's reagent.[27] The assay mixture consisted of phosphate buffer, DTNB and cell extract. The reaction was monitored at 412 nm and the amount of GSH was expressed in terms of nmol GSH/mg protein. Superoxide dismutase (SOD) activity was estimated employing a method described earlier.[28] The assay mixture contained sodium pyrophosphate buffer, nitrobluetetrazolium (NBT), phenazine methosulphate (PMS), reduced nicotinamide adenine dinucleotide (NADH) and the required volume of cell extract. One unit of SOD enzyme activity is defined as the amount of enzyme required for inhibiting the chromogen production (optical density at 560 nm) by 50% in 1 minute under assay conditions and expressed as specific activity in units/minute/mg protein. Catalase (CAT) activity was measured by following its ability to split hydrogen peroxide (H_2O_2) within 1 minute of incubation time. The reaction was then stopped by adding dichromate/acetic acid reagent, and the remaining H_2O_2 was determined by measuring chromic acetate at 570 nm which is formed by reduction of dichromate/acetic acid in the presence of H_2O_2 as described earlier.[29] CAT activity was expressed as μmol H_2O_2 decomposed/minute/mg protein.

Caspase-3 and caspase-9 assays

Activity of caspase-3 and caspase-9 enzymes was measured in A549 cells treated with different concentrations of ZnO nanorods and soluble Zn^{2+} using standard kit (BioVision, Inc.). This assay is based on the principle that activated caspases in apoptotic cells cleave the synthetic substrates to release free chromophore p-nitroanilide (pNA), which is measured at 405 nm. The pNA was generated after specific action of caspase-3 and caspase-9 on tertrapeptide substrates DEVD-pNA and LEHD-pNA, respectively. The reaction mixture consisted of 50 μl of cell extract protein (50 μg), 50 μl of 2× reaction buffer (containing 10 mM dithiothreitol) and 5 μl of 4 mM DEVD-pNA (for caspase-3) or LEHD-pNA (for caspase-9) substrate in a total volume of 105 μl. The reaction mixture was incubated at 37°C for 1 hour and absorbance of the product was measured using microplate reader (Synergy-HT, BioTek) at 405 nm according to manufacturer's instruction.

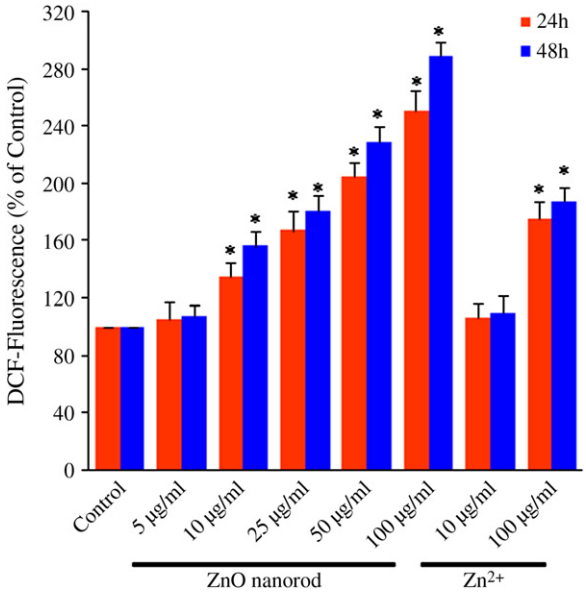

Figure 3. Comparative effects of ZnO nanorods and Zn^{2+} on intracellular ROS generation in human alveolar adenocarcinoma cells. Cells were treated with 5, 10, 25, 50 and 100 μg/ml of ZnO nanorods and 10 and 100 μg/ml of Zn^{2+} for 24 and 48 h. At the end of treatment ROS level was measured as described in the Methods section. Data represented are mean ± SD of three identical experiments made in triplicate. *Statistically significant difference as compared to the controls ($P < 0.05$ for each).

Western blot analysis

For western blot analysis cells were cultured in 6-well plates and exposed to ZnO nanorods at the concentration of 100 μg/mL for 24 h. The harvested cell pellets were lysed in RIPA lysis buffer [1× TBS (0.5M Tris-HCl and 1.5M NaCl) pH 7.4, 1% NP-40, 0.5% sodium deoxycholate, 0.1% SDS, 0.004% sodium azide] in the presence of a protease inhibitor cocktail. The cell lysates were then analyzed for protein content using SDS-PAGE immunoblotting. The membrane was then probed with antibodies to determine levels of protein expression. The following dilutions of primary and secondary antibodies were used: anti-p53 (1:1000, Sigma-Aldrich #P7874), anti-survivin (1:500, Sigma-Aldrich #S8191), anti-bax (1:400, Sigma-Aldrich #B8429), anti-bcl-2 (1:500, Sigma-Aldrich #2521), anti-β-Actin (1:3000, Sigma-Aldrich #A1978) and goat anti-mouse IgG-HRP (1:3000, Santa

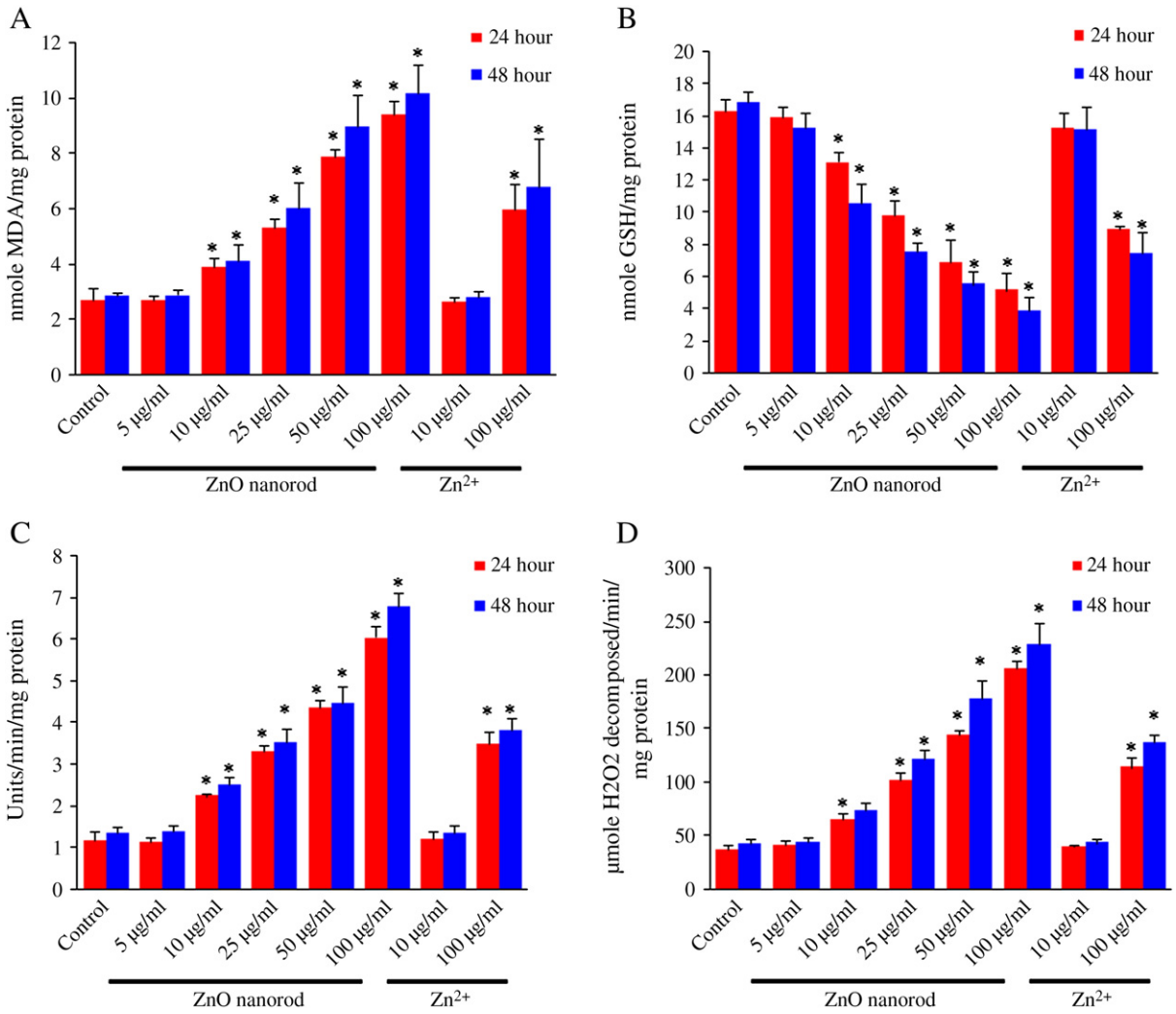

Figure 4. Comparative effects of ZnO nanorods and Zn^{2+} on the biomarkers of oxidative stress in human alveolar adenocarcinoma cells. Cells were treated with 5, 10, 25, 50 and 100 µg/ml of ZnO nanorods and 10 and 100 µg/ml of Zn^{2+} for 24 and 48 h. At the end of treatment oxidative stress biomarkers were determined as described in the Methods section. **(A)** MDA level, **(B)** GSH level, **(C)** CAT activity and **(D)** SOD activity. Data represented are mean ± SD of three identical experiments made in triplicate. *Statistically significant difference in comparison with the controls ($P < 0.05$ for each).

Cruz #sc-2005) and goat anti-rabbit IgG-HRP (1:3000, Santa Cruz #sc-2004).

Protein estimation

Estimation of protein was done using a bicinchoninic acid (BCA) protein assay kit (Pierce Biotechnology, Inc., Rockford, Illinois). This kit is a detergent-compatible formulation based on BCA for the colorimetric detection and quantification of total protein.

Statistical analysis

Statistical significance was determined by one-way analysis of variance (ANOVA) followed by Dunnett's multiple comparison test. Significance was ascribed at $P < 0.05$. All analyses were conducted using the Prism software package (GraphPad Software Inc., La Jolla, California).

Results

Characterization of ZnO nanorods

Figure 1, *A* shows the XRD pattern of prepared ZnO nanorods that clearly exhibits the crystalline nature of this material. The crystallite size has been estimated from the XRD pattern using the Scherrer's equation.[30]

$$D = \frac{0.9\lambda}{B\cos\theta}$$

[where D is the grain size, λ the wavelength of x-ray (1.54056 Å), B the full width at half maxima of the diffraction peak (in radian)].

The average crystallite size corresponding to the highest peak observed in XRD was found to be 50 nm. The presence of sharp structural peaks in XRD patterns and average crystallite size less than 100 nm suggested the nano-crystalline nature of the particles. Figures 1, *B* and *C* show the typical SEM and

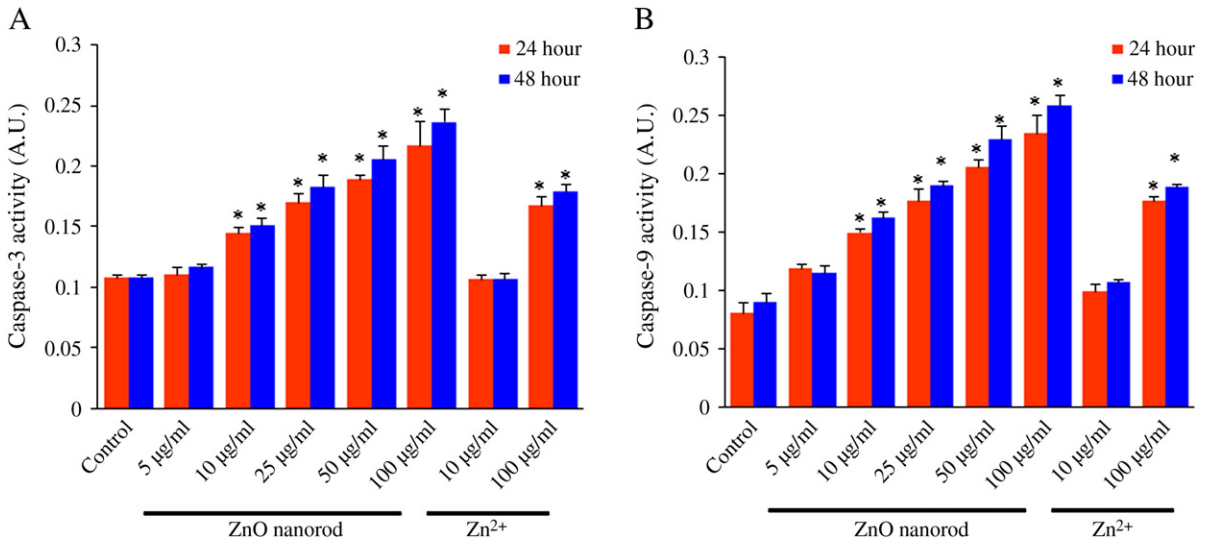

Figure 5. Comparative effects of ZnO nanorods and Zn^{2+} on the activity of caspase-3 and caspase-9 enzymes in human alveolar adenocarcinoma cells. Cells were treated with 5, 10, 25, 50 and 100 μg/ml of ZnO nanorods and 10 and 100 μg/ml of Zn^{2+} for 24 and 48 h. At the end of treatment enzymes activity were determined using BioVision kit as described in the Methods section. **(A)** Caspase-3 activity and **(B)** caspase-9 activity. Data represented are mean ± SD of three identical experiments made in triplicate. *Statistically significant difference i comparison with the controls ($P < 0.05$ for each).

TEM images of the nanoscale ZnO particles, respectively. These pictures show that the majority of the particles were in rod shape with smooth surfaces and monodispersity. TEM average diameter was calculated from measuring over 100 particles in random fields of TEM view. The average TEM diameter of ZnO nanorods was 52 nm further supporting the XRD result. Figure 1, *D* represents the frequency of TEM size distribution of ZnO nanorods. The aspect ratio of ZnO nanorods used in this study is obtained by dividing the mean length of the major axis with the mean width of minor axis (n = 100). The average aspect ratio of ZnO nanorods was 2.88. The EDX spectrum of ZnO nanorods is given in Figure 1, *E*. An oxygen peak at about 0.52 keV and Zn signals at about 1 keV and 8.6 keV were observed in the spectra. The presence of Cu signal was from the Cu grid used. The EDX result showed that there were no other elemental impurities present in ZnO nanorods used in this study.

All of the data from electron microscopy and associated techniques was obtained under high vacuum and constitutes the size, morphology, electron diffraction and composition analysis characteristics of the ZnO nanorods. However, once the ZnO nanorods were introduced cell culture media, the sizes changed to approximately 2 times the primary size. The average hydrodynamic size and zeta potential of the ZnO nanorods suspension in cell culture medium determined by DLS was 97 nm and -29 mV, respectively (Figure 1, *F*). The higher size of NPs in aqueous suspension in comparison with TEM and XRD sizes might be due to the tendency of particles to aggregate in aqueous state. This finding is supported by other investigators and has been briefly discussed in our previous publications.[10,11,14,31]

ZnO nanorod induced cytotoxicity

We examined the mitochondrial function (MTT reduction) and membrane damage (LDH leakage) as cytotoxicity end points. MTT results demonstrated a time- and concentration- dependent cytotoxicity after exposure to ZnO nanorods in A549 cells (Figure 2, *A*). The MTT reduction observed after 24 hours of exposure at the concentrations of 10, 25, 50, and 100 μg/ml was 73%, 60%, 49%, and 41%, respectively, with a further reduction to 61%, 48%, 38% and 27% after 48 hours' exposure. ZnO nanorod was also found to induce LDH leakage in a time- and dose-dependent manner (Figure 2, *B*). A linear correlation was also observed between LDH leakage and MTT reduction (Figure 2, *C*).

ZnO nanorod induced oxidative stress

Higher production of intracellular ROS led to cellular oxidative stress, which has been cited to be one of the more important mechanisms of toxicity related to NP exposure.[32,33] The potential of ZnO nanorods to induce oxidative stress was assessed by measuring the ROS, LPO, GSH, SOD and CAT in A549 cells. Results showed that ZnO nanorod induced the intracellular production of ROS in a time- and dose-dependent manner (Figure 3). ZnO nanorod-induced oxidative stress was further evidenced by depletion of GSH and induction of LPO, SOD and CAT with time and concentrations of ZnO nanorods (Figures 4, *A, B, C* and *D*).

ZnO nanorod induced the activity of caspase-3 and caspase-9 enzymes

Apoptosis refers to programmed cell death in response to various intrinsic or extrinsic death signals, and is executed by series of cysteine proteases known as caspases.[34] Caspase-9 activation is dependent on the release of cytochrome c from mitochondria to form the apoptosome, which in turn activates caspase-3. In this study, significant higher activity of caspase-3 and caspage-9 enzymes was observed in a time- and dose-dependent manner (Figures 5, *A* and *B*) that suggest the involvement of caspase cascade in ZnO nanorod-induced apoptosis in A549 cells.

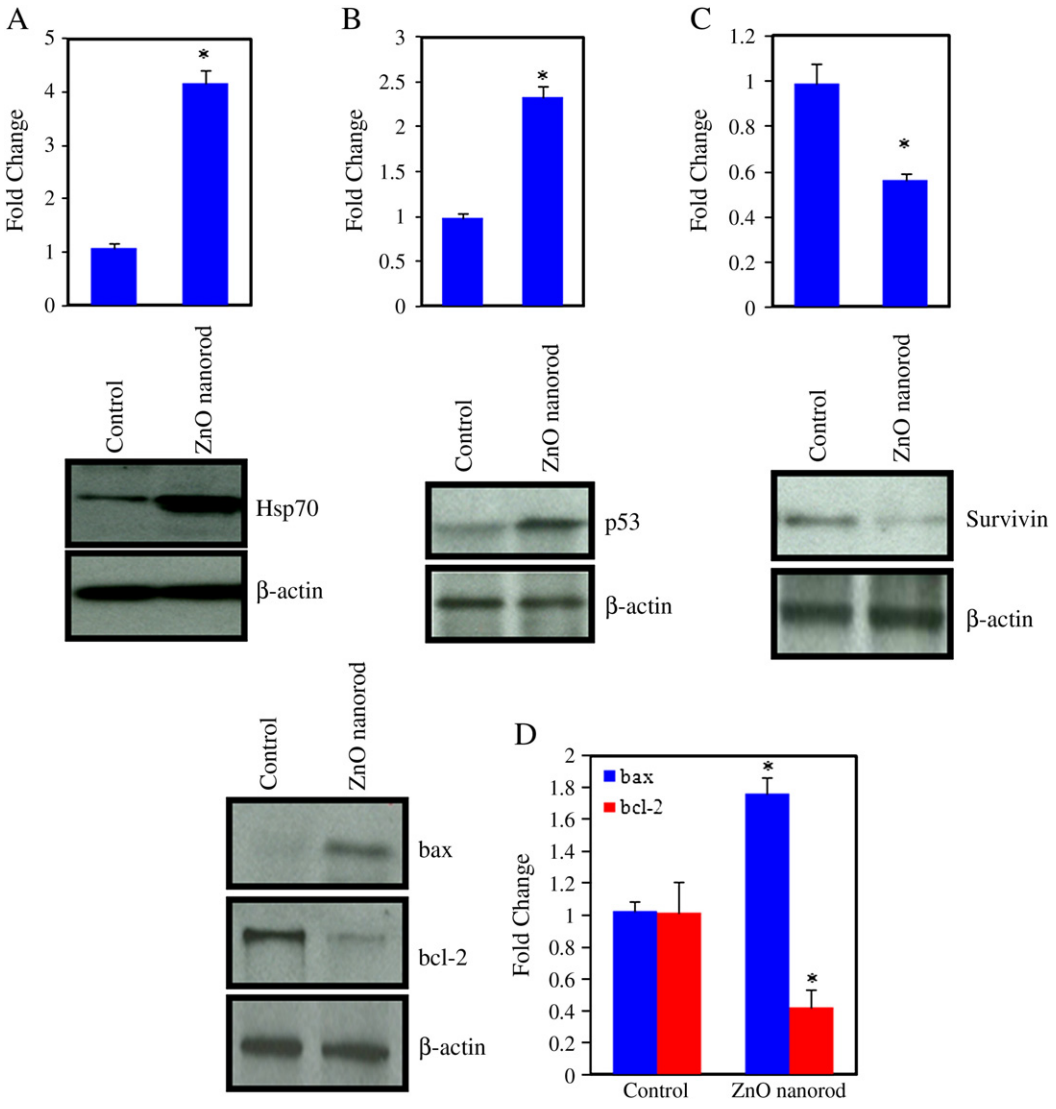

Figure 6. ZnO nanorod induced Hsp70, p53, survivin, bax and bcl-2 protein expression levels in human alveolar adenocarcinoma cells. Cells were treated with ZnO nanorods at a concentration of 100 μg/ml for 24 h. The treated and untreated cells were lysed in RIPA buffer and cell extract subjected to western blots with anti-Hsp70 and anti-p53 antibody as described in the Methods section. Immunoblot images are the representative of 3 identical experiments. The β-actin blot is a loading control. Protein levels were analyzed by desitometric analysis using AlphaEase TM FC StandAlone V.4.0.0 software. Results are also expressed as a fold change over the control group. Bar diagrams are from mean ± SD of 3 blots. *Statistically significant difference in comparison with the controls ($P < 0.05$ for each). **(A)** Hsp70, **(B)** p53 protein **(C)** survivin protein **(D)** bax/bcl-2 proteins.

Dissolution of ZnO nanrods into Zn^{2+} and effects of soluble Zn^{2+} on mitochondria function, lactate dehydrogenase leakage, oxidative stress, apoptosis markers

To determine whether our observed cytotoxicity, oxidative stress and apoptosis could be attributed to the released Zn^{2+}, we analyzed the level of Zn^{2+} released from ZnO nanorods and tested the effect of this defined concentration of Zn^{2+} in A549 cells. The released Zn^{2+} concentrations in the ZnO nanorods suspension at the end of exposure were measured, and the highest dissolution of 10.23 ± 0.41 μg/ml released Zn^{2+} was found in 100 μg/ml ZnO nanorods suspension. Furthermore, the released Zn^{2+} concentrations in 5, 10, 25 and 50 μg/ml ZnO nanorods treatments were 0.43 ± 0.05, 0.89 ± 0.23, 2.33 ± 0.27 and 4.90 ± 0.43 μg/ml, respectively. Our data on the dissolution of ZnO nanoparticles in aqueous state are in agreement with other recent studies.[10,11]

Keeping in view the fact that 10 μg/ml soluble Zn^{2+} present in the 100 μg/ml of ZnO nanorods suspension, we examined the toxic effect of 10 μg/ml of soluble Zn^{2+} in A549 cells and found that Zn^{2+} caused no apparent cytotoxicity (MTT reduction and LDH leakage), oxidative stress (ROS, LPO, GSH, CAT and SOD) and apoptosis (caspase-3 & -9). These results suggest that toxicity observed by ZnO nanorods (in the concentration range 10-100 μg/ml) was due solely to ZnO nanorods, not soluble Zn^{2+}. We further examined the toxic effects of 100 μg/ml of soluble Zn^{2+} and found that higher concentration of Zn^{2+} exerted toxicity, but their effect was less significant in comparison with

the similar concentrations of ZnO nanorods, as shown in Figures 2, 3, 4, and 5. Taken together, our data highlight the differences between ZnO nanorods and soluble Zn^{2+} in causing cytotoxicity and oxidative stress and apoptosis in A549 cells.

ZnO nanorods modulate the expression of proteins involved in DNA damage and apoptosis

We utilized the western blot analysis to see the effect of ZnO nanorods on DNA damage and apoptosis markers in A549 cells exposed to ZnO nanorods at a concentration of 100 μg/ml for 24 hours. The result showed that expression of Hsp70, a first-tier biomarker of cellular damage, was significantly higher in ZnO nanorod-treated cells in comparison with untreated control cells (Figure 6, *A*). The expression level of p53 protein, a cell-cycle checkpoint protein was significantly higher in cells treated with ZnO nanorods (Figure 6, *B*). The expression level of survivin, a fascinating protein that acts as an inhibitor of apoptosis was lower in ZnO nanorods treated cells (Figure 6, *C*). We further examined the effect of ZnO nanorods on bcl-2 and bax proteins. These are two members of the bcl-2 family that play a prominent role in the regulation of apoptosis. Results showed that the expression of bcl-2 (antiapoptotic protein) was significantly lower and the expression of bax (pro-apoptotic protein) was significantly higher in the cells exposed to ZnO nanorods (Figure 6, *D*). Higher expression level of bax/bcl-2 proteins ratio in cells treated with ZnO nanorods suggests that these 2 proteins also play a significant role in the pathway of ZnO nanorod-induced apoptosis.

Discussion

ROS generation and cellular oxidative stress have been cited as possible mechanisms of NPs' toxicity.[32] Our results also show that ZnO nanorods induced cytotoxicity and oxidative stress in human alveolar adenocarcinoma A549 cells. ZnO nanorods induced the generation of ROS in treated cells. MDA level, a marker of LPO, was significantly higher and antioxidant GSH level was significantly lower in ZnO nanorod-treated cells. Antioxidant enzymes SOD and CAT levels were also significantly higher in the cells exposed to ZnO nanorods. The depletion of GSH in ZnO nanorods-exposed cells combined with the increased level of ROS, LPO, SOD and CAT, suggesting that oxidative stress might be the primary mechanism for toxicity of ZnO nanorods in A549 cells. Our results are consistent with previous studies suggesting that cytotoxcity of nZnO was mediated through ROS generation and oxidative stress.[9,13]

It has been demonstrated that Zn^{2+} released from the surface of nZnO when they were suspended in aqueous state[10,11] Therefore, we examined the degree of ionization of ZnO nanorods in cell culture medium and their effects on cytotoxicity, oxidative stress and apoptosis markers. Atomic absorption spectrometry results showed that the highest dissolution of 10 μg/ml released Zn^{2+} was found in 100 μg/ml ZnO nanorods in cell culture media. Biological data demonstrated that soluble Zn^{2+} at the concentration of 10 μg/ml did not produce significant cytotoxicity, oxidative stress and apoptosis in A549 cells. Our findings are in agreement with earlier in vitro studies demonstrating that nZnO liberate Zn^{2+} ions in aqueous state, but the levels of Zn^{2+} released were insufficient to promote cytotoxicity in human cells unless the particulate matter is in contact with the cells.[35,36] Moreover, in vivo studies were also reported that nZnO was not likely a result solely of particles' dissolution, as soluble Zn^{2+} alone caused much less toxicity to zebrafish embryos than nZnO.[10,11]

Apoptosis is a key process in cancer development and progression. The ability of cancer cells to avoid apoptosis and continue to propagate is one of the basic characteristics of cancer and is a major target of cancer-therapy development.[37] We provided evidence that ZnO nanorods induced apoptosis in human alveolar adenocarcinoma A549 cells. Western blot results showed that the expression of Hsp70, a biomarker of cell damage was induced by ZnO nanorods. ZnO nanorods upregulated the cell cycle checkpoint protein p53 and downregulated the antiapoptotic protein survivin. Investigations have shown that there is a strong association between decreased survivin levels and induction of apoptosis in cancer cells.[17,38] Antiapoptosis function of survivin also seems to be related to the ability to disturb the function of caspases.[38] To support this finding our results also show that ZnO nanorods inhibit the expression of survivin along with activation of caspase-3 and caspase-9 enzymes. Furthermore, expression of antiapototic protein bcl-2 was significantly lower, and the expression of pro-apoptotic protein bax was significantly higher in cells exposed to ZnO nanorods, suggesting that these proteins could be excellent molecular biomarkers to assess the apoptotic response of NPs.[39] Our results are consistent with other investigators' findings that demonstrated metal oxide NPs have the potential to induce apoptotic cell death.[22,30-42]

In conclusion, we demonstrated that ZnO nanorods induced cytotoxicity, oxidative stress and apoptosis in human alveolar adenocarcinoma cells. The expressions of cell-cycle checkpoint protein p53 and pro-apoptotic protein bax were upregulated, and the antiapototic proteins, survivin and bcl-2, were downregulated by ZnO nanorods. Activity of caspase-3 and caspase-9 enzymes was also induced in ZnO nanorod-treated cells. These results suggest that ZnO nanorod induced apoptosis in human alveolar adenocarcinoma cells via p53, survivin, bax/bcl-2 and caspase pathways mediated by oxidative stress through which most of the chemotherapeutic drugs trigger apoptosis.

References

1. Wang ZL. Splendid one-dimensional nanostructures of zinc oxide: a new nanomaterial family for nanotechnology. ACS Nano 2008;2:1987-92.
2. Yuranova T, Laub D, Kiwi J. Synthesis, activity and characterization of textiles showing self-cleaning activity under daylight irradiation. Catal Today 2007;122:109-17.
3. Serpone N, Dondi D, Albini A. Inorganic and organic UV filters: their role and efficacy in sunscreens and sun-care products. Inorg Chim Acta 2007;360:794-802.
4. Hanley C, Layne J, Punnoose A, Reddy KM, Coombs I, Coombs A, et al. Preferential killing of cancer cells and activated human T cells using ZnO nanoparticles. Nanotechnology 2008;19:295103 (10pp).
5. Ostrovsky S, Kazimirsky G, Gedanken A, Brodie C. Selective cytotoxic effect of ZnO nanoparticles on glioma cells. Nano Res 2009, doi:10.1007/s12274-009-9089-5.
6. Premanathan M, Karthikeyan K, Jeyasubramanian K, Manivannan G. Selective toxicity of ZnO nanoparticles toward Gram positive bacteria

and cancer cells by apoptosis through lipid peroxidation. Nanomedicine 2010, doi:10.1016/j.nano.2010.10.001.
7. Deng X, Luan Q, Chen W, Wang Y, Wu M, Zhang H. Et al. Nano-sized zinc oxide particles induce neural stem cell apoptosis. Nanotechnology 2009;18:115101 (8pp).
8. Berardis BD, Civitelli G, Condello M, Lista P, Pozzi R, Arancia G, et al. Exposure to ZnO nanoparticles induces oxidative stress and cytotoxicity in human colon carcinoma cells. Toxicol Applied Pharmacol 2010;246: 116-27.
9. Huang CC, Aronstam RS, Chen DR, Huang YW. Oxidative stress, calcium homeostasis, and altered gene expression in human lung epithelial cells exposed to ZnO nanoparticles. Toxicol in Vitro 2010;24: 45-55.
10. Bai W, Zhang Z, Tian W, He X, Ma Y, Zhao Y, et al. Toxicity of zinc oxide nanoparticles to zebrafish embryo: a physicochemical study of toxicity mechanism. J Nanopart Res 2009;12:1645-54.
11. Zhu X, Wang J, Zhang X, Chang Y, Chen Y. The impact of ZnO nanoparticle aggregates on the embryonic development of zebrafish (*Danio rerio*). Nanotechnology 2009;20:195103 (9pp).
12. Kahru A, Dubourguier HC. From ecotoxicology to nanoecotoxicology. Toxicology 2010;269:105-19.
13. Xia T, Kovochich M, Liong M, Madler L, Gilbert B, Shi H, et al. Comparison of the mechanism of toxicity of zinc oxide and cerium oxide nanoparticles based on dissolution and oxidative stress properties. ACS Nano 2008;2:2121-34.
14. Sharma V, Shukla RK, Saxena N, Parmar D, Das M, Dhawan A. DNA damaging potential of zinc oxide nanoparticles in human epidermal cells. Toxicol Lett 2009;185:211-8.
15. Lin W, Xu Y, Huang CC, Ma Y, Shannon KB, Chen DR, et al. Toxicity of nano- and micro-sized ZnO particles in human lung epithelial cells. J Nanopart Res 2009;11:25-39.
16. Farnebo M, Bykov VN, Wiman KG. The p53 tumor suppressor: a master regulator of diverse cellular processes and therapeutic target in cancer. Biochem Biophys Res Commun 2010;396:85-9.
17. Li HL, Ma AN. Induction of apoptosis of non-small cell lung cancer by a methylated oligonucleotide targeting survivin gene. Canc Gene Ther 2010;17:441-6.
18. Reed JC. Proapoptotic multidomain bcl-2/bax family proteins: mechanisms, physiological roles and therapeutic opportunities. Cell Death Different 2006;13:1378-86.
19. Liu JJ, Huang RW, Lin DJ, Peng J, Wu XY, Lin Q, et al. Expression of survivin and bax/bcl-2 in peroxisome proliferator activated receptor-g ligands induces apoptosis on human myeloid leukemia cells in vitro. Annals of Oncol 2005;16:455-9.
20. Raja M, Shanmugaraj AM, Ryu SH. Preparation of template free zinc oxide nanoparticles using sol-gel chemistry. J Nanosci Nanotech 2008;8:4224-6.
21. Chen Q, Wang Y, Xu K, Lu G, Ying Z, Wu L, et al. Curcumin induces apoptosis in human lung adenocarcinoma A549 cells through a reactive oxygen species-dependent mitochondrial signaling pathway. Oncol Rep 2010;2:397-403.
22. Ahamed M, Siddiqui MA, Akhtar MJ, Ahmad I, Pant AB, Alhadlaq HA. Genotoxic potential of copper oxide nanoparticles in human lung epithelial cells. Biochem Biophys Res Commun 2010;396:578-83.
23. Mossman T. Rapid colorimetric assay for cellular growth and survival: application to proliferation and cytotoxicity assays. J Immunol Meth 1983;65:55-63.
24. Akhtar MJ, Ahamed M, Kumar S, Siddiqui H, Patil G, Ashquin M, et al. Nanotoxicity of pure silica mediated through oxidant generation rather than glutathione depletion in human lung epithelial cells. Toxicology 2010;276:95-102.
25. Wang H, Joseph JA. Quantifying cellular oxidative stress by dichlorofluorescein assay using microplate reader. Free Radic Biol Med 1999;27: 612-6.
26. Ohkawa H, Ohishi N, Yagi K. Assay for lipid peroxides in animal tissues by thiobarbituric acid reaction. Anal Biochem 1979;95:351-8.
27. Ellman Gl. Tissue sulfhydryl groups. Arch Biochem Biophys 1959;82: 70-7.
28. Kakkar PS, Das B, Viswanathan PN. A modified spectrophotometric assay of superoxide dismutase. Ind J Biochem Biophys 1984;21:130-2.
29. Sinha AK. Colorimetric assay of catalase. Anal Biochem 1972;47:389-94.
30. Patterson AL. The Scherrer formula for x-ray particle size determination. Phys Rev 1939;56:978-82.
31. Ahamed M, Posgai R, Gorey TJ, Nielsen M, Hussain S, Rowe J. Silver nanoparticles induced heat shock protein 70, oxidative stress and apoptosis in *Drosophila melanogaster*. Toxicol Appl Pharmacol 2010;242:263-9.
32. Nel A, Xia T, Madler L, Lin N. Toxic potential of materials at the nano level. Science 2006;311:622-7.
33. Ahamed M, AlSalhi MS, Siddiqui MKJ. Silver nanoparticle applications and human health. Clin Chim Acta 2010;411:1841-8.
34. Fadeel B, Orrenius S. Apoptosis: a basic biological phenomenon with wide-ranging implications in human disease. J Intern Med 2005;258: 479-517.
35. Gojova A, Guo B, Kota RS, Rutledge JC, Kennedy IM, Barakat AI. Induction of inflammation in vascular endothelial cells by metal oxide nanoparticles: effect of particle composition. Environ Health Perspect 2007;115:403-9.
36. Moos PJ, Chung K, Woessner D, Honeggar M, Cutler NS, Veranth JM. ZnO particulate matter requires cell contact for toxicity in human colon cancer cells. Chem Res Toxicol 2010;23:733-9.
37. Ashkenazi A. Targeting death and decoy receptors of the tumor-necrosis factor superfamily. Nat Rev Cancer 2002;2:420-30.
38. Zaffaroni N, Pannati M, Diadone MG. Survivin as a target for new anticancer interventions. J Cell Mol Med 2007;9:360-72.
39. Zhu L, Chang DW, Dai L, Hong Y. DNA damage induced by multiwalled carbon nanotubes in mouse embryonic stem cells. Nano Lett 2007;7:3592-7.
40. Ahamed M, Karns M, Goodson M, Rowe J, Hussain S, Schlager J, et al. DNA damage response to different surface chemistry of silver nanoparticles in mammalian cells. Toxicol Appl Pharmacol 2008;233:404-10.
41. Eom HJ, Choi J. Oxidative stress of CeO_2 nanoparticles via p38-Nrf-2 signaling pathway in human bronchial epithelial cell, Beas-2B. Toxicol Lett 2009;187:77-83.
42. Kang SJ, Kim BM, Lee YJ, Hong SH, Chung HW. Titanium dioxide nanoparticles induce apoptosis through the JNK/p38-caspase-8-bid pathway in phytohemagglutinin-stimulated human lymphocytes. Biochem Biophys Res Commun 2009;386:682-7.